Finite Volume Errors in B_K

Jangho Kim[*]**, Hyung-Jin Kim, Weonjong Lee**

Lattice Gauge Theory Research Center, CTP, and FPRD,
Department of Physics and Astronomy, Seoul National University, Seoul, 151-747, South Korea
E-mail: wlee@snu.ac.kr

Chulwoo Jung

Physics Department, Brookhaven National Laboratory, Upton, NY11973, USA
E-mail: chulwoo@bnl.gov

Stephen R. Sharpe

Physics Department, University of Washington, Seattle, WA 98195-1560, USA
E-mail: sharpe@phys.washington.edu

SWME Collaboration

We discuss finite volume errors in our calculations of B_K using improved staggered fermions on the MILC asqtad lattices. Using GPUs, we are now able to extrapolate using next-to-leading order (NLO) staggered SU(2) chiral perturbation theory including the finite volume corrections arising from pion loops. We find that the impact of FV fitting is very small, giving a 0.5% shift in the continuum limit.

---

[*]Speaker.

---

1. Introduction

The dominant error in our calculation of B_K using improved staggered quarks [1] comes from our use of a truncated matching factor, but a significant subdominant error is that from extrapolating from finite to infinite volume. In our earlier work we estimated this error by comparing the results on two volumes. Here we describe an alternative estimate using next-to-leading order (NLO) chiral perturbation theory (ChPT). Specifically, we replace the pion loop integrals with their finite volume form, perform the chiral fit, and then use the fit parameters to determine the result in infinite volume. This method is fairly standard in chiral fits, but, given our large data set, has been too expensive to implement at the desired accuracy until recently. Using GPUs we can now incorporate the finite volume (FV) corrections into the fitting routines using $SU(2)$ staggered ChPT. First results were presented in Ref. [2], and here we present an update.

2. Finite Volume Effects in SU(2) staggered chiral perturbation theory

Finite volume corrections enter at NLO in SU(2) ChPT only through the chiral logarithms arising from loops of pions composed of valence $\bar{d}$ and d quarks. The standard chiral logarithmic functions that enter are

$$\ell(X) = X\left[\log(X/\mu_{\mathrm{DR}}^2) + \delta_1^{\mathrm{FV}}(X)\right], \tag{2.1}$$

$$\tilde{\ell}(X) = -\frac{d\ell(X)}{dX} = -\log(X/\mu_{\mathrm{DR}}^2) - 1 + \delta_3^{\mathrm{FV}}(X), \tag{2.2}$$

where μ_{DR} is the scale introduced by dimensional regularization, and X is squared mass (in physical units) of the $\bar{d}d$ pion. The functions $\delta_1^{FV}(X)$ and $\delta_3^{FV}(X)$ contain the finite volume corrections:

$$\delta_1^{\mathrm{FV}}(M^2) = \frac{4}{ML}\sum_{n\neq 0}\frac{K_1(|n|ML)}{|n|} \tag{2.3}$$

$$\delta_3^{\mathrm{FV}}(M^2) = 2\sum_{n\neq 0}K_0(|n|ML), \tag{2.4}$$

where M is the pion mass, L is the box size in the spatial direction, K_1 and K_0 are modified Bessel functions, and $n = (n_1, n_2, n_3, n_4)$ is a image vector in 4-dimension lattice. The norm $|n|$ is

$$|n| \equiv \sqrt{n_1^2 + n_2^2 + n_3^2 + \left(\frac{L_T}{L}n_4\right)^2} \tag{2.5}$$

where L_T is the Euclidean temporal box size.
The details are explained in Ref. [1].

3. Numerical Study

In order to calculate the finite volume corrections δ_1^{FV} and δ_3^{FV} in Eqs. (2.3-2.4), we use the following criteria to truncate the sum over n. For δ_1^{FV}, with desired precision $\varepsilon = 1.0 \times 10^{-14}$ (double precision), we first determine $r_{\max}$ from

$$[4\pi r_{\max}^2] \times \frac{K_1(r_{\max}ML)}{r_{\max}} = \varepsilon \times [6K_1(ML)]. \tag{3.1}$$

Here, $4\pi r_{\max}^2$ is the density of image vectors at $|n| = r_{\max}$ and $6K_1(ML)$ is the contribution to δ_1^{FV} from the first set of images with $|n| = 1$. In words, we keep images out to a distance $r_{\max}$ at which the contribution from a shell of radius $\Delta r = 1$ equals the desired precision times the leading contribution from $|n| = 1$. We assume in this estimate that $L_T \gg L$ (with L_T the extent in the temporal direction), so that we only consider spatial images. This is the source of the factor of 6 multiplying $K_1(ML)$. Similarly for δ_3^{FV}, we define $r_{\max}$ from

$$[4\pi r_{\max}^2] \times K_0(r_{\max}ML) \geq \varepsilon \times [6K_0(ML)]. \tag{3.2}$$

In the second step, we define spatial and temporal "radii" through

$$r_s = r_{\max}, \qquad r_t = \frac{L}{L_T} \times r_{\max}. \tag{3.3}$$

Finally, when we calculate the finite volume corrections Eq. 2.3 and Eq. 2.4, we include only images satisfying

$$\begin{aligned} -r_s \leq n_i \leq r_s \qquad &\text{for} \qquad i = 1,2,3 \\ -r_t \leq n_4 \leq r_t \end{aligned} \tag{3.4}$$

Therefore, the number of the image vectors n is essentially $(2r_s + 1)^3 \times (2r_t + 1)$.

To draw plots of B_K vs. pion mass-squared X, we calculate finite volume corrections for about hundred different mass values. The radius $r_{\max}$ varies with X, but roughly we find we need, for 100 different mass values in the relevant range, about 10^9 image vectors. Since there are about 1000 configurations in each ensemble, we need about 10^{12} evaluations of Bessel functions per ensemble. If we use a standard CPU to calculate finite volume corrections for all the MILC asqtad ensembles that we have data on, it takes about two months. This is clearly impractical, and we need significantly faster computational resources. GPUs provide the solution to this problem.

4. CUDA Programming

GPUs are composed of many tiny multi-processors which can handle the single instruction multiple data efficiently. We use Nvidia GTX480 GPUs which have a peak speed of 168 giga flops in double precision [3]. We use CUDA for GPU programming and obtain 64.3 giga flops (38% of the peak) in double precision. This is almost 120 times faster than the CPU code (0.5 giga flops). We use the following optimization techniques.

- Substituting Division by Multiplication:
  Division is slower than multiplication in GPU calculation. For example, the division operation $x/4$ is much slower than the multiplication operation $x \times 0.25$. After this optimization, we get 16% gain in the speed.

- Coalesced Access:
  Coalesced access allows sequential threads to access sequential GPU memories in parallel. Coalesced access is at least twice as fast as uncoalesced access. We find that including coalesced access in the global sum algorithm leads to a 20% gain.

5. Results

We use MILC asqtad ensembles listed in Table 1. They are generated with $N_f = 2+1$ flavors of asqtad staggered sea quarks. The values of light sea quark masses (am_l) and strange sea quark

Table 1: MILC lattices used for the numerical study. Here, "ens" represents the number of gauge configurations, "meas" is the number of measurements per configuration, and ID will be used later to identify the corresponding lattice.

a (fm)	am_l/am_s	size	ens $\times$ meas	ID
0.12	0.03/0.05	$20^3 \times 64$	564×9	C1
0.12	0.02/0.05	$20^3 \times 64$	486×9	C2
0.12	0.01/0.05	$20^3 \times 64$	671×9	C3
0.12	0.01/0.05	$28^3 \times 64$	275×8	C3-2
0.12	0.007/0.05	$20^3 \times 64$	651×10	C4
0.12	0.005/0.05	$24^3 \times 64$	509×9	C5
0.09	0.0062/0.031	$28^3 \times 96$	995×9	F1
0.09	0.0031/0.031	$40^3 \times 96$	850×1	F2
0.06	0.0036/0.018	$48^3 \times 144$	744×2	S1
0.06	0.0025/0.018	$56^3 \times 144$	198×9	S2
0.045	0.0028/0.014	$64^3 \times 192$	705×1	U1

masses (am_s) are given in Table 1. We use four different lattice spacings: coarse ($a = 0.12$ fm), fine ($a = 0.09$ fm), superfine ($a = 0.06$ fm), and ultrafine ($a = 0.045$ fm) lattices.

In our numerical study on B_K, we use HYP-smeared staggered fermions as valence quarks. HYP staggered fermions have a number of advantages such as reducing taste symmetry breaking as efficiently as HISQ action [4]. We use 10 different values of the valence quark masses (m_x for the d quark and m_y for the $\bar{s}$) as given in Table 2.

Table 2: Valence quark masses (in lattice units).

a (fm)	am_x and am_y	
0.12	$0.005 \times n$	with $n = 1, 2, 3, \ldots, 10$
0.09	$0.003 \times n$	with $n = 1, 2, 3, \ldots, 10$
0.06	$0.0018 \times n$	with $n = 1, 2, 3, \ldots, 10$
0.045	$0.0014 \times n$	with $n = 1, 2, 3, \ldots, 10$

In Table 3, we present our results for B_K with and without including finite volume (FV) terms in the fitting, as well as the difference between the two. Note that the differences are statistically significant despite the fact that the error in the individual results is larger than the difference. This is because the two fits are highly correlated. We find very small shifts, indicating that FV effects are a subpercent systematic. We also note that the impact of including FV corrections on our largest lattice (C3-2) is negligible, indicating that this volume is effectively infinite.

Table 3: $B_K(\mathrm{NDR}, 1/a)$ with finite volume corrections. The results are obtained by extrapolation to physical down quark mass and removing lattice artifacts due to taste breaking. The second column gives the results from extrapolation using the infinite volume SU(2) staggered ChPT form. The third column gives results from fitting to the FV form, and then removing the FV corrections from the final number. The last column gives the percentage change. The fit type is 4X3Y-NNLO of the SU(2) analysis, which is explained in Ref. [1]. am_y is fixed to the heaviest quark mass (for example, $am_y = 0.05$ for the C3 ensemble).

ID	B_K	B_K(FV)	ΔB_K
C3	0.5734(46)	0.5743(46)	+0.16%
C3-2	0.5784(46)	0.5785(46)	+0.02%
F1	0.5074(37)	0.5049(37)	-0.49%
S1	0.4914(65)	0.4898(65)	-0.33%
U1	0.4812(65)	0.4790(65)	-0.46%

We now display some of the fits that lead to these numbers. Figures 1(a), 1(b), 2(a), 2(b) and 3(a) show "X-fits" on the C3, C3-2, F1, S1 and U1 ensembles, respectively. The red line denotes fitting without finite volume corrections and the blue line denotes those with FV corrections included. The diamonds give B_K obtained, as explained above, by extrapolating $m_x \to m_d^{\mathrm{phys}}$, setting all pion taste-splittings to zero, and (in the case of the FV fit) setting $L, L_T \to \infty$.

(a) C3 ensemble   (b) C3-2 ensemble
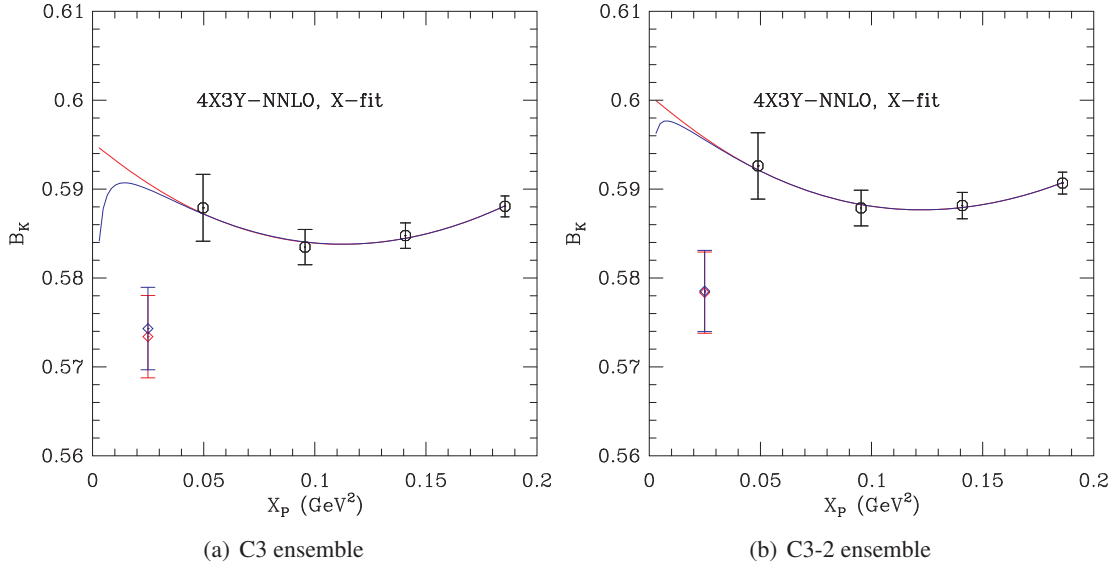
Figure 1: $B_K(1/a)$ vs. X. The left figure shows results from the C3 ensemble, while the right figure shows results from the C3-2 ensemble. The fit type is 4X3Y-NNLO in the SU(2) analysis [1]. We fix $am_y = 0.05$. The red line represents the results of fitting with no finite volume correction. The blue line corresponds to those with finite volume corrections included. The diamonds correspond to the B_K value obtained by extrapolating m_x to the physical light valence quark mass after setting all the pion taste-splittings to zero.

Fig. 3(b) compares the continuum extrapolation with and without the finite volume corrections. The total correction in the continuum limit is 0.46%.
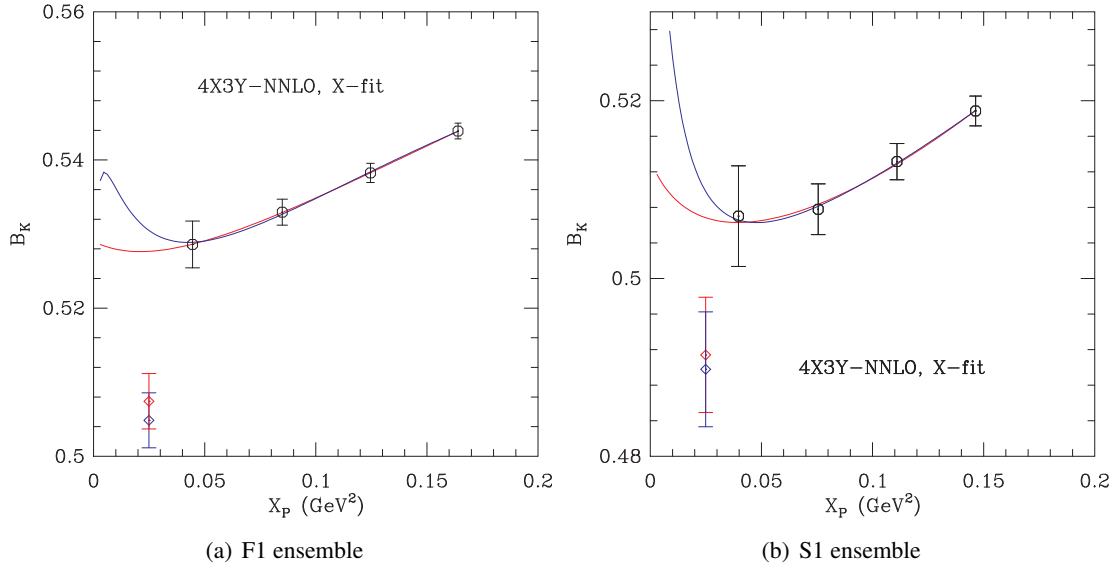
(a) F1 ensemble

(b) S1 ensemble

Figure 2: $B_K(1/a)$ vs. X. The left figure shows results from the F1 ensemble and the right figure from the S1 ensemble. The fit type is 4X-NNLO in the SU(2) analysis [1].
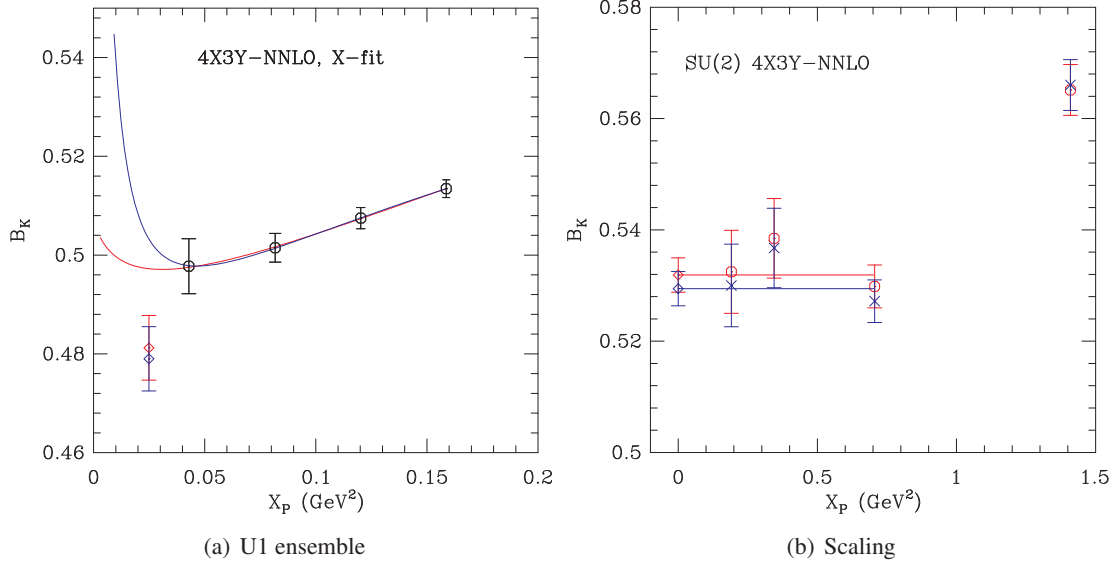

(a) U1 ensemble

(b) Scaling

Figure 3: The left figure shows $B_K(1/a)$ vs. X for the U1 ensemble. The fit type is 4X-NNLO in the SU(2) analysis. The right figure shows $B_K(2\text{GeV})$ vs. a^2. The red octagons show data obtained using the SU(2) fitting without the finite volume corrections. The blue crosses show results from SU(2) fitting with the FV corrections incorporated. Diamonds show the results after extrapolation to the continuum ($a = 0$) using the smallest three values of a.

6. Conclusion

By using GPUs, we have significantly reduced the computational time for FV corrections in NLO chiral expressions. This has made it practical to fit and extrapolate using the FV-corrected forms. Using this method we have updated all our SU(2) staggered ChPT fits, with results reported in Ref. [5].

We find the FV effect to be at the subpercent level, although, as shown in the figures for the finest ensembles, FV effects would get much larger if we lowered the valence quark masses any further.

Comparing the results from Table 3 from the C3 and C3-2 ensembles, we see that the FV shift on the C3 lattice is significantly smaller than difference between the central values from the two lattices. There is no inconsistency here because the errors on individual lattices are large enough that we cannot statistically distinguish between the results on the two volumes. Because of this, we think that the FV shift based on ChPT is a more reliable estimator of the FV systematic, and we use this in our updated results.

7. Acknowledgments

References

[1] Taegil Bae, *et al.*, SWME Collaboration, Phys. Rev. D**82**, (2010), 114509; [arXiv:hep-lat/1008.5179].

[2] Jangho Kim, *et al.*, SWME Collaboration, Phys. Rev. D**83**, (2011), 117501; [arXiv:hep-lat/1101.2685].

[3] Hyung-Jin Kim and Weonjong Lee, SWME Collaboration, PoS (Lattice 2010) 230 ; [arXiv:hep-lat/1010.4782].

[4] Taegil Bae and David H. Adams and Chulwoo Jung and Hyung-Jin Kim and Jongjeong Kim and Kwangwoo Kim and Weonjong Lee and Stephen R. Sharpe, SWME Collaboration, Phys. Rev. D**77**, (2008), 094508 ; [arXiv:0801.3000].

[5] Weonjong Lee, *et al.*, SWME Collaboration, PoS (Lattice 2011) 316 ; [arXiv:hep-lat/1110.2576].